Journal of Advanced Marine Engineering and Technology, Vol. 45, No. 2, pp. 70~78, 2021
J. Advanced Marine Engineering and Technology (JAMET)
https://doi.org/10.5916/jamet.2021.45.2.70

ISSN 2234-7925 (Print)
ISSN 2765-4796 (Online)
Original Paper

Study on LNG cold energy recovery using combined refrigeration and ORC system: LNG-fueled refrigerated cargo carriers

Bo Rim Ryu[1] · Duong Phan Anh[2] · Yoon Hyeok Lee[3] · Ho Keun Kang†

(Received February 23, 2021 ; Revised March 26, 2021 ; Accepted April 20, 2021)

Abstract: This study simulated the conversion of the existing aged refrigerated cargo carriers into liquefied natural gas (LNG)-fueled ships to comply with the International Maritime Organization emission regulations. A useful method for the recovery of LNG cold energy, which is generated from the process of LNG vaporization and causes ecosystem disturbances owing to its low temperature when released into the sea, is presented in the study. The proposed method consists of two systems. One is an indirect refrigeration system with ethyl alcohol for the preservation of tuna as brine refrigerant instead of a multi-press refrigeration system with R22, and the other is a power generation system using the organic Rankine cycle (ORC). Considering a refrigeration cargo hold that consumes 256 kW of power for its operation, the refrigeration system based on LNG cold energy consumes approximately 7 kW of power for its operation; thus, it can save approximately 198 kW of power when compared with the power consumed by a conventional refrigeration system. Additionally, the ORC power generation system based on LNG cold energy can produce up to 17 kW of power using R134b under optimal conditions. This power saving of 215 kW represents a cost-effective and environmentally friendly way to save fuel and environmental costs because it can reduce diesel generator operating times.

Keywords: LNG, Cold energy, Refrigerated cargo carriers, Indirect refrigeration system, ORC

1. Introduction

The tightening of emission regulations by the International Maritime Organization (IMO)**[1]** has led to a continued increase in demand for large vessels and passenger liners that use liquefied natural gas (LNG) as a fuel. Additionally, to address the environmental concerns, there is ongoing research on the application of LNG-fueled systems. However, there is a distinct lack of research on LNG-based propulsion for small- and medium-size cargo ships. Jafarzadeh *et al.***[2]** report that the size of refrigerated cargo carriers tends to be small or medium and outfitted with large refrigeration equipment for handling cargo at temperatures of -20 to -40 °C or lower. According to 2016 statistics from Clarksons research, approximately 42% (342 out of 799) of the refrigerated cargo carriers around the world are more than 30 years old, and 95% of them will inevitably have to be dismantled or destroyed owing to their deterioration.

Under these circumstances, new designs and builds of refrigerated cargo carriers should be based on frameworks that consider the IMO emission regulations. Among the multiple alternatives, the LNG-fueled system is the most reasonable. Therefore, it is necessary to continue research on the application of LNG-fueled systems for refrigerated cargo carriers**[3]**.

In the handbook by Mokhatab *et al.***[4]**, the LNG used as the shipboard fuel is stored in tanks at a temperature of approximately -163 °C, and vaporizers such as the open rack vaporizer, submerged combustion vaporizer, intermediate fluid vaporizer, and shell and tube vaporizer are used to gasify LNG at 45 °C to supply to the engine. In this process, approximately 830–860 kJ/kg of cold energy is released into seawater or air. In the study by He *et al.***[5]**, treating seawater used in LNG evaporation at 10 °C should be considered because seawater can disturb marine ecosystems. Industrial applications of LNG cold energy include the direct use of cold energy by constructing a plant close to the LNG station for exchanging the cold energy to the cryogenic LNG and the indirect use of the cold energy by transporting it to a remote location via a tank lorry. The types of the cold energy

† Corresponding Author (ORCID: http://orcid.org/0000-0003-0295-7079): Professor, Division of Coast Guard Studies, Korea Maritime & Ocean University, 727, Taejong-ro, Yeongdo-gu, Busan 49112, Korea, E-mail: hkkang@kmou.ac.kr, Tel: +82-51-410-4260
1 Ph. D. Candidate, Division of Marine System Engineering, Korea Maritime & Ocean University, E-mail: ryuborim@g.kmou.ac.kr, Tel: +82-51-410-4862
2 Ph. D. Candidate, Division of Marine System Engineering, Korea Maritime & Ocean University, E-mail: anhdp.qhqt@gmail.com, Tel: +82-51-410-4862
3 Assistant Research Engineer, R&D Center, DongHwa Entec, E-mail: lyh@dh.co.kr, Tel: +82-51-970-0716

use in the industry includes direct applications, such as air liquefaction separation**[6][7]**, desalination**[8][9]**, liquefied carbonic acid production**[10][11]**, refrigerated warehousing**[12][13]**, and electric energy generation**[14][15]**, and indirect applications, such as low-temperature grinding and food freezing, with practical use found mainly in Japan. The temperatures utilized by industries that employ LNG cold energy range from 0 °C low-temperature states for low-temperature refrigeration and low-temperature cultivation to -200 °C cryogenic states for hydrogen liquefaction and cryogenic power transmission facilities.

Exergy can be understood as the maximum amount of useful work that can be gained from the stream/gas when it reaches an equilibrium condition with the reference environment while interacting only with this environment and the high exergy use can be in gas liquefaction separation, cold energy storage, and so on **[16]**. If these studies on LNG cold energy utilization**[17][18]** were to be applied to vessels with LNG-fueled propulsion, it would be a significant technological development that would contribute to the prevention of environmental pollution and the growth of green energy.

The low-temperature power cycle in the power generation system is one of the most desirable ways to use the LNG low-temperature energy. LNG can be used to replace the coolant with a heat sink in the energy cycle. The basic cryogenic power cycles using LNG low-temperature energy are direct expansion cycles, organic Rankine cycles (ORCs), and Brayton cycles. The direct expansion cycle is a special cycle because it uses only the mechanical exergy (pressure exergy) of LNG. In the direct expansion cycle, LNG is pumped to a designated pressure above the pipeline distribution pressure and then regasified to natural gas in the LNG vaporizer. The high-pressure natural gas then generates power by reducing the pressure to equilibrate with the pipeline distribution pressure in the turbine**[14]**. However, cold energy is still wasted in this cycle. Therefore, direct expansion cycles are always combined with other cycles to improve the efficiency of overall power generation. The Kalina cycle is considered a potential cycle for recovering LNG cold energy **[19]**.

The ORC uses working fluids that operate at low temperatures to recover LNG low-temperature energy from the condenser. In the ORC system, the working fluid generates power through compression, evaporation, expansion, and condensation, using LNG as a heat sink during the condensation process. Choi *et al.***[14]** focused on the selection of working fluids and the construction of cycles to maximize the utilization of cold energy in ORCs for utilizing LNG cold energy. Chen *et al.***[15]** investigated the optimization of three ORC configurations, namely, single-stage ORC, parallel two-stage ORC (PTORC), and cascade two-stage ORC, to utilize LNG cold energy and reduce heat. They adopted eight potential working fluids to maximize the exergy efficiency and optimize the ORC at the configuration level. The optimization results indicated that PTORC achieved a maximum exergy efficiency of 17.36% using an ammonia/ethane working fluid at 50 °C. Qiu *et al.***[20]** pointed out that the cascade multi-stage ORC system maximizes the utilization of LNG low-temperature energy. When the number of steps increases, the net power, energy efficiency, and excitation efficiency of the system increase. However, the greater the number of stages, the more complex the system. Therefore, a three-stage ORC with a cascade configuration is recommended.

In this study, LNG cold energy refrigeration systems and ORC generators were connected to the fuel supply system of an existing LNG-fueled ship. The LNG cold energy conditions were analyzed through simulations. The effects of LNG cold energy on the efficiency of the refrigeration system were analyzed. Furthermore, the efficiency of the proposed system was compared with those of the existing refrigeration systems. The optimum working fluid was selected by comparing the characteristics of working fluids for a power generation system utilizing LNG cold energy.

2. System Modeling and Simulation

2.1 Conditions and State Equations

In this study, it was assumed that the LNG-fueled system was installed on a 3,300-ton-class refrigerated cargo carrier transporting frozen tuna, as depicted in **Figure 1**. The vessel information and the specifications of the LNG-fueled system are listed in **Table 1**.

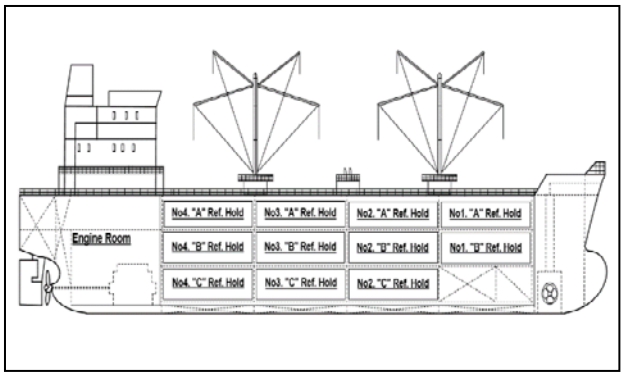

Figure 1: 3,300-ton-class refrigerated cargo carrier

The design and analysis of the system were performed using HYSYS ver. 11.0, a process simulation software from Aspen Technology Inc. For the equation of state, the Peng–Robinson equation was chosen for the LNG and other fluids used in the process. The Peng–Robinson equation **[21]** is capable of quantitative liquid-state volume calculations and is widely used in equilibrium calculations for hydrocarbons. Therefore, we do not explain this equation here.

Table 1: Specifications of refrigerated cargo carrier and LNG-fueled system

Item		Specification
Type of cargo		Tuna (−60 °C)
Cargo hold volume		4,370 m^3
Quantity of heat(Heat capacity)		256 kW
M/E	Model	Wärtsila 9L20DF
	Sets	3 sets
	Type	4 strokes DFDE
	Output	1,665 kW/set
Fuel	Flow rate	1,522 kg/h
	Initial temp.	−163 °C
	Initial pressure	1.0 bar
	Engine inlet temp.	45 °C
	Engine inlet pressure	6 bars

*DFDE: dual-fuel diesel electric

2.2 Design of Refrigeration System Utilizing LNG Cold Energy

To utilize LNG cold energy, an indirect refrigeration system using brine refrigerant was used in this study. **Figure 2** shows a schematic of the proposed indirect refrigeration system utilizing LNG cold energy. LNG was pumped using a low-pressure pump located inside the LNG tank. In heat exchange No. 1, the working fluid of the brine refrigeration system released heat to the LNG and its temperature was decreased. Next, it was provided to each cargo hold for refrigerant missions. After heat transfer in the vaporizer, the vaporized natural gas (NG), which had a temperature of -80 °C and pressure of 6 bar, was supplied to the HC separator, where heavy hydrocarbon components were separated and discharged. Subsequently, the natural gas at 6 bar and -80 °C was provided to the second heat exchanger, where received heat to increase its temperature to 45 °C before being supplied to the combustion chamber of the dual-fuel engine.

The produced boil-off gas (BOG) of a natural gas service tank was also utilized to feed the engine. The BOG at 0.2 bar and -160 °C was compressed using a low-pressure compressor to obtain the gas at 6 bar and 60 °C. Then, it was cooled using a gas cooler to obtain the same conditions as that of the natural gas after heat exchange No. 02 at 6 bar and 45 °C, before being supplied to the engine.

In comparison with a direct cooling system, the indirect refrigeration system has the advantages of being simple, small, easy to maintain, and low investment costs. There are also the added benefits of improved freshness and greater stability of food items in the refrigerator, because there is no risk of leakage during the compression and expansion processes. The brine refrigerant used in refrigeration systems should have the properties of high specific heat, low viscosity, low specific gravity, low freezing point, and low corrosiveness to metals. For this study, ethyl alcohol, a brine refrigerant often used in environments with temperatures below -50 °C, was chosen. Additionally, evaporated NG was passed through a heavy hydrocarbon separator to ensure that only NG with a methane number of 80 or greater was supplied to the feed line to prevent the occurrence of the methane slip with dual-fuel engines using NG with a methane number lower than 80. A schematic of the refrigeration system utilizing LNG cold energy is shown in **Figure 2**.

The following assumptions were made for the simulation to run on HYSYS.

- The compression process is an adiabatic compression process, and the compression and mechanical efficiencies of the pump are 0.85.
- The expansion process of the cycle is an isenthalpic process.
- The pressure drops and heat loss of the refrigerant in the heat exchanger (condenser and evaporator) were ignored.
- The state of the LNG after passing through the evaporator was -85 °C and 7 bar.

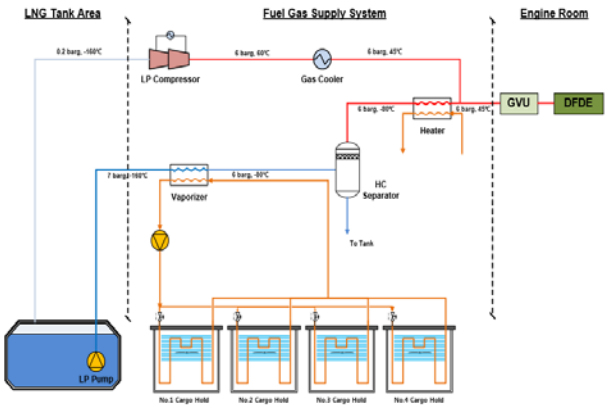

Figure 2: Schematic of the refrigeration system using LNG cold energy

Table 2: Typical composition of the LNG fuel at -163 °C, -85 °C, and boiling points of compositions

Temperature	-163 °C	-85 °C	Boiling point at 1bar
Composition	Mole %	Mole %	
Methane (CH_4)	90.91	93.26	-161°C
Ethane (C_2H_6)	6.43	5.76	-88.6°C
Propane (C_3H_8)	1.66	0.63	-42.1°C
i-Butane (C_4H_{10})	0.74	0.08	-0.5°C
Nitrogen (N_2)	0.26	0.27	-195°C
Methane number	75	84	-

To maintain a methane number above 80, which is the engine manufacturer's recommendation for fuel gas, the temperature of LNG was raised, and methane with a low boiling point and some ethane were first boiled owing to the difference in the boiling points of the major components. A temperature of − -85 °C was chosen because NG has a methane number of 84 at this temperature, which satisfies the minimum methane number required by the low–medium pressure engine **[22]**. The compositions of LNG at -163 °C, -85 °C, and the boiling points of the compositions are listed in **Table 2**.

The coefficient of performance of a brine utilizing an indirect refrigeration system (COP_{Brine}) was calculated using the equation below:

$$COP_{Brine} = \frac{Q_e}{W_{Pump}} \quad (1)$$

2.3 Power Generation System Utilizing LNG Cold Energy

The power generation system consisted of an initial heat exchange from the refrigeration cycle condenser to reach a temperature of -85 °C, followed by heating to approximately 45 °C via a secondary heat exchanger connected to an ORC generator to satisfy the temperature requirement for a methane number of 84 or greater required by the dual-fuel engine. The steam from the boiler was also used as the heat source for the evaporator and heater. The schematic of the power generation system is shown in **Figure 3**.

The assumptions made for the simulation were as follows.

- The compression process is an adiabatic compression process, and the compression and mechanical efficiencies of the pump are 0.85.
- The expansion process of the turbine is an isenthalpic process.
- The pressure drops and heat loss of the working fluid in the heat exchanger (condenser and evaporator) were ignored.
- The work output from the ORC generator system, Wnet, and its cycle efficiency, ηth, were calculated using the following equations:

$$W_{net} = W_{turbine} - W_{pump} \quad (2)$$

$$\eta_{th} = \frac{W_{net}}{Q_{evap}} \quad (3)$$

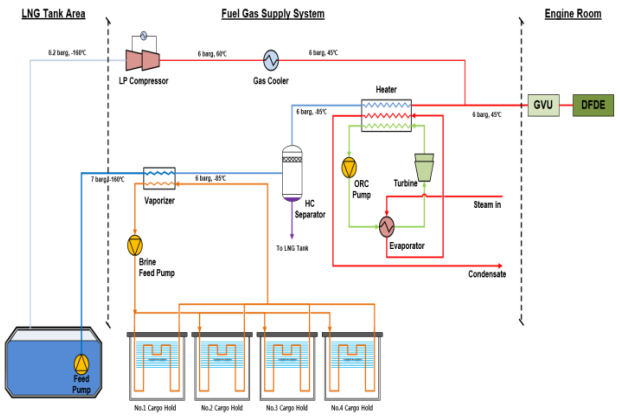

Figure 3: Schematic of the concept design for power generation

The exergy efficiency of the ORC generator, η_{II}, was calculated by applying the second law of thermodynamics using the following equations **[23]**:

$$\eta_{II} = \eta_{th}\,(1 - \frac{T_L}{T_H})^{-1} \quad (4)$$

$$T_H = \frac{T_{steam_{in}} + T_{PP}}{2} \quad (5)$$

$$T_L = \frac{T_{NG\_in} + T_{NG\_out}}{2} \quad (6)$$

The selected working fluid is a factor that significantly affects the efficiency of the ORC, a constituent of the power generation system. Our selection criteria for working fluids for the ORC system include environmental friendliness, safety, and high working performance. Among these, working fluids with eco-friendly properties of the ODP of zero (0), GWP of less than 2500, and atmospheric lifetime of less than 20 year were considered. For the safety criteria, low toxicity and low flammability working fluids from the A1 and A2 groups of the American Society of

Heating, Refrigerating, and Air-Conditioning Engineers (ASHRAE) standards were chosen **[14]**. From this group, R236ea, which does not have an ASHRAE safety rating, is regarded as a nontoxic and nonflammable fluid, whereas R245fa is chosen owing to its widespread use as a working fluid for the ORC system despite its safety rating of B1 **[15][20]**. The properties of the five working fluids selected and applied in this study using the aforementioned selection criteria are listed in **Table 3**.

3. Results and Discussions

For reference, the change in work done by the evaporator and pump depending on the amount of usable LNG cold energy according to the LNG evaporation temperature is shown in **Figure 4**. The curve shown in the figure indicates the impact of the LNG vaporizing temperature on the working power of the evaporator. Thus, when the LNG vaporizing temperature (increasing the amount of LNG through the vaporizer) increased, the work performed by the vaporizer increased and the work of the refrigeration system also increased, whereas the work performed by the pump remained unchanged. In other words, the amount of cold energy and work performed by the refrigeration system is significantly affected by the temperature of the LNG through the vaporizer, whereas the pump's work remains unaffected.

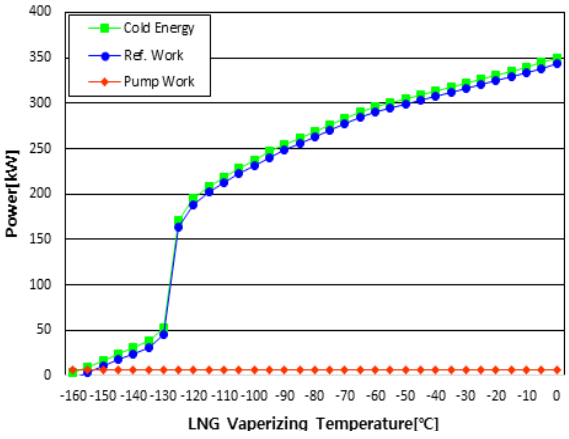

Figure 4: Variation in power of evaporator and pump with LNG vaporizing temperature

3.1 Parametric Analysis of ORC Power Generation System

3.1.1 Impact on Condensation Temperature

Condensation temperature is very important for the system efficiency in ORC design. This is because the turbine operation energy is proportional to the difference between the condensation and evaporation temperatures. The simulation conditions were set with a fixed turbine inlet temperature of 90 °C, and the condensation temperature was changed from − -30 °C to 0 °C in 5 °C increments. As a result, there was a tendency for the net power output to increase with an increase in the condensation temperature, as shown in **Figure 5**.

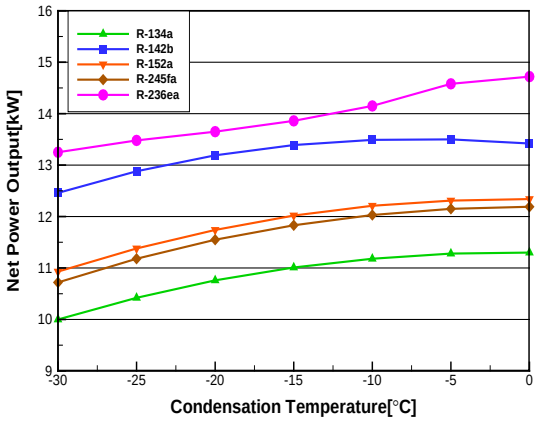

Figure 5: Variation in net power output with condensation temperature

This demonstrates the impact of the net power output of each working fluid on condensation temperature. Therefore, by increasing the inlet temperature of the turbine, the power generation of the ORC system by R-134a, R-152a, R245fa, and R236ea tended to gradually increase, whereas R-142b gradually decreased from -10 °C onward. The net power output increased with an increase in the condensation temperature from -30 °C to -15 °C and a relatively trivial change from -15 °C to 0 °C. When the condensation temperature is lower than -15 °C, the mass flow rate increases. Thus, the power generated by the ORC turbine increased proportionally. However, as stated in the assumption for the simulation, the turbine inlet temperature was set at 90 °C, and

Table 3: Properties of working fluid at 1 atm

Working Fluid	ODP	GWP	ALT	Safety Class	Boiling Temperature [°C]	Critical Temperature [°C]	Critical Pressure [bar]
R134a	0	1300	13.8	A1	-26.1	101.1	40.67
R142b	0	2400	19	A2	-9.0	131.1	41.23
R152a	0	124	1.4	A2	-14	113.0	45.17
R245fa	0	950	4.7	B1	15.3	154.0	36.51
R236ea	0	1200	8	N.A	-1.4	139.0	34.20

the natural gas temperature in and out of the heater was set at -85 °C and 45 °C, respectively. This means that the heat source temperature was set, and the total heat exchange in this heater was unchanged. Thus, the increase in mass flow rates tended to decrease with an increase in the condensing temperature; therefore, the change in the power output of the system was relatively trivial.

However, owing to the total heat gained from the evaporator increasing with an increase in condensation temperature, as shown in **Figure 6** and **Figure 7**, respectively, the thermal and exergy efficiencies of the ORC decreased with an increase in the condensation temperature, based on equations (4)-(6).

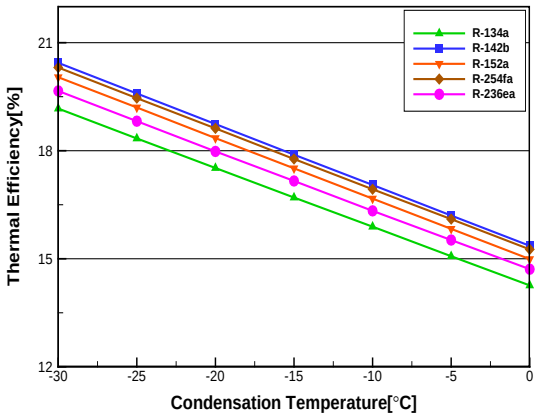

Figure 6: Variation in thermal efficiency with condensation temperature

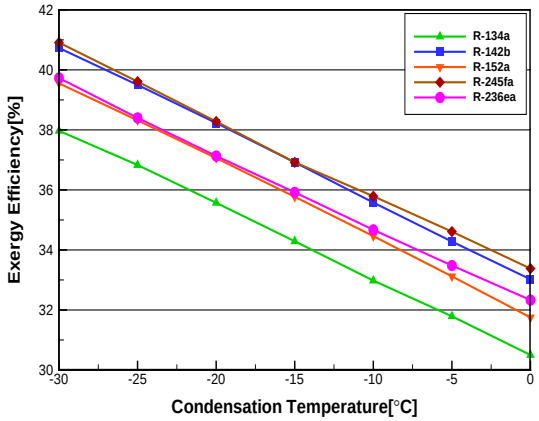

Figure 7: Variation in exergy efficiency with condensation temperature

3.1.2 Impact on Pressure Variation at Turbine Inlet

The ORC performance was analyzed at various turbine inlet pressures, between 10 and 30 bar, with the inlet temperature fixed at 90 °C and the condensation temperature set to -30 °C, which showed the highest efficiency in the aforementioned performance analysis of the cycle at various condensation temperatures.

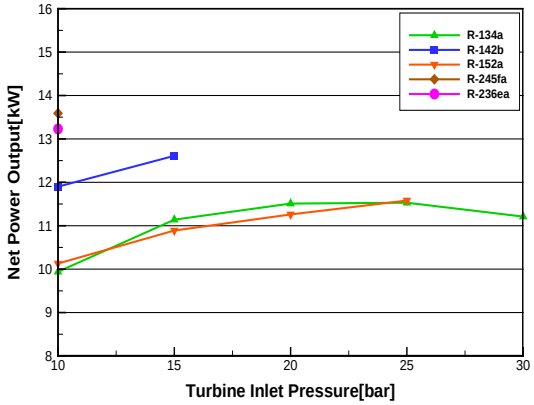

Figure 8: Variation in net power output with turbine inlet pressure

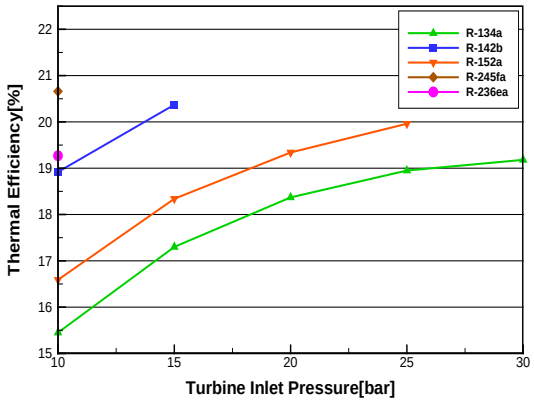

Figure 9: Variation in thermal efficiency with turbine inlet pressure

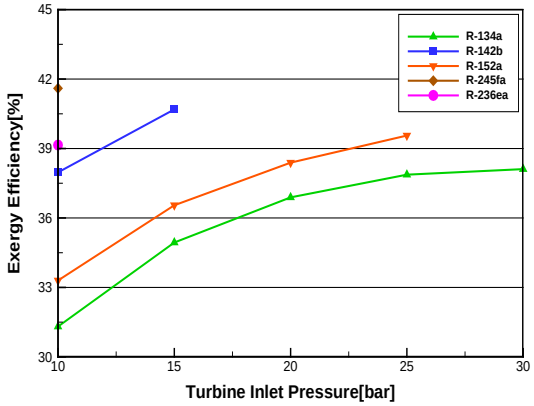

Figure 10: Variation in exergy efficiency with turbine inlet pressure

The results of the analysis indicated that as the turbine inlet pressure increased, the net power output (as depicted in **Figure**

8) and efficiency (as depicted in **Figures 9** and **10)** improved. However, with the exception of R134a, the working fluids were unable to operate cycles at increased pressures because the working fluids changed their state from saturated steam to wet steam, making it impossible to drive the turbine.

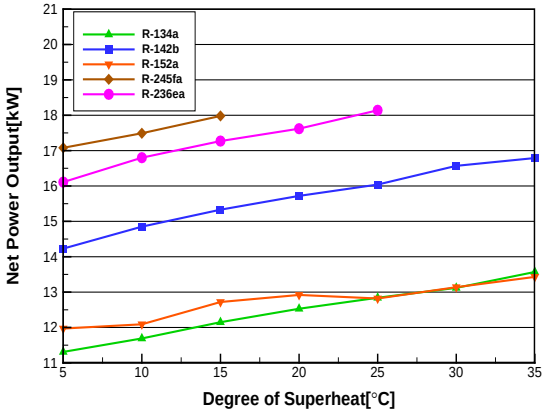

Figure 11: Variation in net power output with the degree of superheat

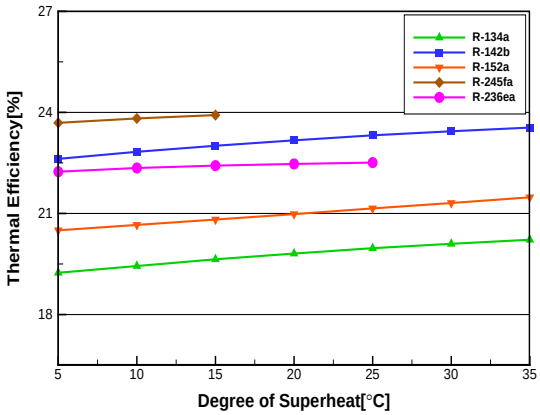

Figure 12: Variation in thermal efficiency with the degree of superheat

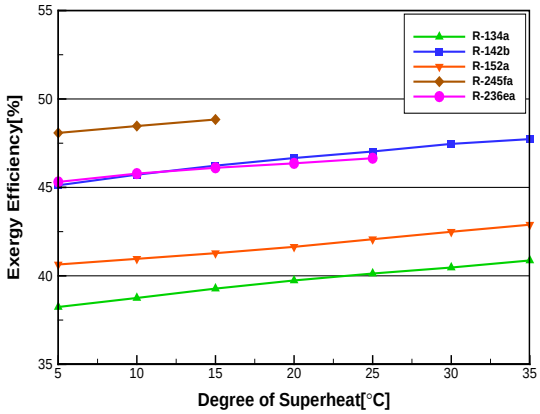

Figure 13: Variation in exergy efficiency with the degree of superheat

3.1.3 Impact on Superheat

Superheat in the ORC is a factor that can affect the thermodynamic aspect of the cycle and cause phase changes in the working fluid. For this reason, the performance of the ORC was analyzed with the superheat temperature raised between 5 °C and 35 °C at intervals of 5 °C and with the condensation temperature and turbine inlet pressure set to 0 °C and 30 bar, respectively, in consideration of the critical pressure of the working fluid.

The analysis of the results indicated that the total power output, thermal efficiency, and exergy efficiency (as depicted in **Figures 11**, **12**, and **13**, respectively) improved as superheating increased. R245fa and R235ea were unable to drive the turbine at superheating temperatures higher than 20 °C and 30 °C, respectively. This was because of the steam temperature of the evaporator, which is the source of heat for increasing superheat, being lower than the superheating boiling temperature of the working fluid, thereby resulting in a wet steam state.

3.2 Performance Analysis of Economic Feasibility

The indirect refrigeration system utilizing LNG was able to save approximately 198 kW of power when compared with the multistage compression refrigeration system using R22 operating a refrigeration cargo hold requiring 256 kW. In addition, by operating the ORC power generation cycle using the cold energy remaining from the first-stage evaporation, approximately 17 kW of additional power could be produced. Through the utilization of cold energy resulting from LNG changing the temperature from − -162°C to 45°C during supply, it was possible to save 215 kW of power. Furthermore, the overall operation time of the diesel generator could be reduced by approximately 30% when compared with the standard operation time, thereby reducing emissions by 30%.

4. Conclusion

This study investigated the application of the basic information of currently operational refrigerated cargo carriers to design and simulate a system that utilizes waste LNG cold energy, which could otherwise cause disturbance to the marine ecosystem if dumped into the ocean, from an LNG-fueled propulsion system to operate the refrigeration system and generate additional energy via ORC. The results of this study were as follows:

1) For a 3,300-ton-class refrigerated cargo carrier with a 4,370 m^3 refrigerated volume, 256 kW of refrigeration power are required to maintain a temperature of -60 °C for the cargo

of frozen tuna. In this scenario, a standard R22 refrigerant-utilizing multistage compression refrigeration system consumes approximately 205 kW of power, whereas utilizing cold energy provides 250 kW of power as LNG, at -162 °C, evaporates to NG at -85°C, ensuring that the ethylene glycol refrigerant-utilizing indirect refrigeration system consumes only 7 kW, leading to a power saving of 198 kW over conventional refrigeration systems.

2) An ORC power generation system could produce an additional 17 kW of power by utilizing approximately 32 kW of cold energy arising from the secondary heat exchanger as -85 °C NG was supplied to the engine at 45 °C NG. The net power output, thermal efficiency, and exergy efficiency of the ORC were found to be affected by changes in the working fluid type, condensation temperature, turbine inlet pressure, and superheat. As a result, it was deemed more appropriate to assess the efficiency of the cold heat recovery system based on exergy efficiency rather than thermal efficiency. Finally, the highest performance (net output of 17 kW, exergy efficiency of 47%) was observed when using the working fluid R-142b at a condensation temperature of -30 °C, turbine inlet pressure of 30 bar, and superheat of 35 °C.

3) When using the two LNG cold energy-utilizing systems, it was possible to conserve 198 kW of power from the refrigeration system and 17 kW of power from the generator, leading to a total power saving of 215 kW. These results indicate that diesel generators onboard the vessels can reduce operation times. Furthermore, the reduced diesel generator operation time and no low-temperature seawater outflow to the ocean owing to the lack of seawater in the LNG evaporation causes this system to be highly eco-friendly.

Acknowledgement

This research was supported by the project “Test evaluation for LNG bunkering equipment and development of test technology(Grant No. 20180048)” funded by the Ministry of Oceans and Fisheries. This work was also supported by the BB21+ project in 2020.

Author Contributions

Conceptualization, B. R. Ryu and H. K. Kang; Methodology, B. R. Ryu and Y. H. Lee; Software, Y. H. Lee; Validation, B. R. Ryu and H. K. Kang; Formal Analysis, D. P. Anh; Investigation, Y. H. Lee and D. P. Anh; Resources, B. R. Ryu and Y. H. Lee; Data Curation, B. R. Ryu and Y. H. Lee; Writing—Original Draft Preparation, H. K. Kang; Writing—Review & Editing, B. R. Ryu, D. P. Anh, and H. K. Kang; Visualization, D. P. Anh; Supervision, H. K. Kang; Project Administration, Y. H. Lee; Funding Acquisition, H. K. Kang.

References

[1] IMO Marine Environment Protection Committee, 72nd session, http://www.imo.org, Accessed April 20, 2018.

[2] S. Jafarzadeh, N. Paltrinieri, I. B. Utne, and H. Ellingsen, “LNG-fuelled fishing vessels: A systems engineering approach,” Transportation Research Part D: Transport and Environment, vol. 50, pp. 202-222, 2017.

[3] K. Cheenkachorn, C. Poompipatpong, and C. G. Ho, “Performance and emissions of a heavy-duty diesel engine fuelled with diesel and LNG,” Energy, vol. 53, pp. 52-57, 2013.

[4] S. Mokhatab, J. Y. Mark, J. V. Valappil and D. A. Wood, Handbook of liquefied natural gas, Amsterdam, Netherland: Elsevier Science, 2014.

[5] T. He, I. A. Karimi, and Y. Ju, “Review on the design and optimization of natural gas liquefaction processes for onshore and offshore applications,” Chemical Engineering Research and Design, ol. 132, pp. 89-114, 2018.

[6] M. Mehrpooya, M. Kalhorzadeh, and M. Chahartaghi, “Investigation of novel integrated air separation processes, cold energy recovery of liquefied natural gas and carbon dioxide power cycle,” Journal of Cleaner Production, vol. 113, pp. 411-425, 2016.

[7] M. Mehrpooya, M. M. M. Sharifzadeh, and M. A. Rosen, “Optimum design and exergy analysis of a novel cryogenic air separation process with LNG (liquefied natural gas) cold energy utilization,” Energy, vol. 90, Part 2, pp. 2047-2069, 2015.

[8] P. Wang and T. -S. Chung, “A conceptual demonstration of freeze desalination-membrane distillation (FD-MD) hybrid desalination process utilizing liquefied natural gas (LNG) cold energy,” Water Research, vol. 46, no. 13, pp. 4037-4052, 2012.

[9] W. Cao, C. Beggs, and I. M. Mujtaba, “Theoretical approach of freeze seawater desalination on flake ice maker

utilizing LNG cold energy," Desalination, vol. 355, pp. 22-32, 2015.

[10] R. Ben-Mansour, M. A. Habib, O. E. Bamidele, M. Basha, N. A. A. Qasem, A. Peedikakkal, T. Laoui, and M. Ali, "Carbon capture by physical adsorption: Materials, experimental investigations and numerical modeling and simulations-a review," Applied Energy, vol. 161, pp. 225-255, 2016.

[11] M. J. Tuinier, M. van Sint Annaland, G. J. Kramer, and J. A. M. Kuipers, "Cryogenic capture using dynamically operated packed beds", Chemical Engineering Science, vol. 65, no. 1, pp. 114-119, 2010.

[12] P. Mumanachit, D. T. Reindl, and G. G. Nellis, "Comparative analysis of low temperature industrial refrigeration systems," International Journal of Refrigeration, vol. 35, no. 4, pp. 1208-1221, 2012.

[13] A. Messineo and G. Panno, "LNG cold energy use in agro-food industry: A case study in Sicily," Journal of Natural Gas Science and Engineering, vol. 3, no. 1, pp. 356-363, 2011.

[14] Y. S. Choi, Y. H. Lee, H. K. Kang, and T. W. Lim, "Performance analysis of the organic Rankine cycle using LNG cold energy in LNG-fueled ships," Journal of the Korean Society of Marine Engineering, vol. 42, no.7, pp. 524-530, 2018 (in Korean).

[15] H. Chen, D. Y. Goswami, and E. K. Stefanakos, "A review of thermodynamic cycles and working fluids for the conversion of low-grade heat," Renewable and Sustainable Energy Reviews, vol. 14, no. 9, pp. 3059-3067, 2010.

[16] M. S. Khan, I. A. Karimi and D. A. Wood, "Retrospective and future perspective of natural gas liquefaction and optimization technologies contributing to efficient LNG supply: A review," Journal of Natural Gas Science and Engineering, vol. 45, pp. 165-188, 2017.

[17] B. B. Kanbur, L. Xiang, S. Dubey, F. H. Choo, and F. Duan, "Cold utilization systems of LNG: A review," Renewable and Sustainable Energy Reviews, vol. 79, pp. 1171-1188, 2017.

[18] T. He, Z. R. Chong, J. Zheng, Y. Ju, and P. Linga, "LNG cold energy utilization: Prospects and challenges," Energy, vol. 170, pp. 557-568, 2019.

[19] H. Ghaebi, T. Parikhani, and H. Rostamzadeh, "Energy, exergy and thermoeconomic analysis of a novel combined cooling and power system using low-temperature heat source and LNG cold energy recovery," Energy Conversion and Management, vol. 150, pp. 678-692, 2017.

[20] G. Qiu, H. Liu, and S. Riffat, "Expanders for micro-CHP systems with organic Rankine cycle," Applied Thermal Engineering, vol. 31, no. 16, pp. 3301–3307, 2011.

[21] Z. Nasri and H. Binous, "Applications of the Peng-Robinson equation of state using Matlab," Chemical Engineering Education, vol. 43, no. 2, pp. 115-124, 2009.

[22] S. Kuczynski, M. Łaciak, A. Szurlej, and T. Włodek, "Impact of liquefied natural gas composition changes on methane number as a fuel quality requirement," Energies, vol. 13, no. 19, 2020.

[23] J. S. Kim, "A study on the characteristics of an Organic Rankine Cycle for ocean thermal energy conversion according to pinch point analysis and a transcritical Cycle," Master Thesis, Division of Marine System Engineering, Korea Maritime & Ocean University, Republic of Korea, 2017 (in Korean).